RSC Advances

Journal Name

ARTICLE

Preparation of lotus-like hierarchical microstructures on zinc substrate and its wettability study

Huijie Wang,[a] Zhou Yang,[b] Jing Yu,[a] Yizhi Wu,[a] Weijia Shao,[a] Tongtong Jiang,[a] and Xiaoliang Xu [a]*

In this paper, we innovatively propose a facile and controllable way to prepare superhydrophobic Zn/ZnO film on zinc substrate. In this approach, we soak the acid etched Zn substrate in pure warm water, resulting in a formation of hierarchical configuration with micron-sized grooves and nanorods. The lotus-like hierarchical Zn/ZnO micro/nano structure can be acquired and tailored in a wide range of reaction conditions by controlling the reaction temperature and duration. The formation mechanism of the hierarchical structure has been discussed. The wettability of as-modified surfaces has been researched through three aspects: superhydrophobicity, oleophobicity (for oily liquids), and oil/water separation property. What's more, as-prepared superhydrophobic samples show good thermal stability (under 200 °C) and recoverability. This approach offers a potential choice for industrial application of self-cleaning surfaces because of its features such as time-saving, low cost, easy to prepare and so on.

1 Introduction

Superhydrophobic surfaces, with water contact angle (WCA) greater than $150°$ and water sliding angle (WSA) lower than $10°$, are usually inspired by the self-cleaning lotus leaf. While water droplets can't stick on the surface and will spontaneously roll off removing dust particles on the leaf [1]. This kind of special surfaces are eliciting widespread interest for extensive application prospects such as self-cleaning coatings [2], anti-oil contamination [3, 4], oil/water separation [5], anti-drag [6], anti-ice/frost [7], anti-reflection film [8], etc. In general, the wettability of a solid surface is mainly controlled by its surface chemical composition and surface topographic structure. Surface chemical composition determines surface free energy, thus the liquid wettability (i.e., hydrophilicity / hydrophobicity/ oleophobicity / oleophilicity), while the surface topographic structure can amplify these properties based on the Wenzel and modified Cassie equation [9, 10]. The fabrication of hierarchical structures is an effective way for improving the surface wettability. First, the hierarchical structure decreases the contact area between solid and water (or oil) at their interface and causes a higher contact angles (CA); second, the

hierarchical structure decreases the continuity of the three-phase contact line at the solid-liquid interface which induces a low sliding angle (SA) as well as low CA hysteresis [11, 12]. When we modify the hierarchical configuration surface with material whose surface tension lower than water but larger than oil, an oil/water separation interface may be obtained.

ZnO nanowires and its other one dimensional nanostructures, have distinctive features such as excellent electron mobility, controllable morphology and high sensitivity under ambient conditions, etc. These above characteristics contribute to its widespread applications, for instance, photovoltaic device[13, 14], gas sensors[15], biomedical fluorescence detection[16], environmental application[17], light emitting diodes and lasers[18] and so on . Among which, the study of ZnO nanowires in the area of water wettability have been reported by a large amount of literatures. In total, the common used techniques for ZnO nanowires growth include electrochemical deposition[19], chemical etch [20], hydrothermal growth [21, 22], thermal oxidation, plasma enhanced chemical vapor deposition [23], etc. On a Zn surface, ZnO microstructures tend to be formed more easily as

Zn substrate itself being the zinc ion source and the similar crystal structure between Zn and ZnO [20, 24].

In this paper, we introduce a water bath process on an acid etched Zn surface to construct hierarchical structure. The hierarchical Zn/ZnO micro-nano configuration can be acquired and tailored in a wide range of reaction conditions by controlling the water temperature and reaction time during the water bath. Then, Stearic acid or Heptadecafluorodecyltrimethoxy-silane ($C_{13}F_{17}H_{13}O_3Si$, HTMS) are used as surface modifier to study several kinds of wettability. The final hierarchical micro/nano Zn/ZnO surfaces achieve excellent superhydrophobicity or oleophobicity (for oily liquids). Interestingly, on a drilled Zn surface, an oil/water separation experiment has been conducted, and the superhydrophobic interface with periodic holes is endowed with good oil/water separation property. What's more, these superhydrophobic samples present good thermal stability. While some one-step methods have been proposed, the operation is simple, but it needs reaction duration even more than 24 h [25-27]. As a comparison, our approach offers a way to manufacture superhydrophobic material in industrial scale because of its advantages such as time-saving, low cost, easy to prepare and so on.

2 Experimental details

2.1 Materials and chemicals

Zinc sheet (99.9%, 0.25mm thick), ethanol (AR), acetone (AR), hydrochloric acid (HCl, 36.0~38.0%), isopropanol (AR), stearic acid (AR) , n-hexane (AR), diiodomethane (CP), formamide (AR), diethylene glycol (AR), ethylene glycol (AR) and methylene blue trihydrate (BS) were used in the experiments. All reagents were brought from Sinopharm Chemical Regent Co. Ltd. (Shanghai, China). Heptadecafluorodecyltrimethoxy-silane ($C_{13}F_{17}H_{13}O_3Si$, HTMS) was bought from Dow Corning Co. (USA). Deionized water with resistivity of 18.25 MΩ·cm was used in the whole experimental process.

2.2 Preparation of hierarchical microstructure on zinc surfaces and surface modification

Scheme 1 A main experimental process.

The main experimental process is depicted in Scheme 1. In a typical process, zinc sheets were ultrasonically cleaned in acetone and ethanol for 10 min respectively. Then the clean zinc sheets were first etched in 4M hydrochloric acid (HCl) for 10 s and in 1 M HCl for 15 s to acquire a primary microstructure; in a second step, zinc sheet being soaked in warm water to acquire a secondary microstructure. The water bath temperature ranged from 50 ℃ to 90 ℃ and the soaking duration ranged from 0.5 h to 12 h. For comparison, sample with just hydrochloric acid etched has been prepared.

One contrast experiment was conducted to study the just water bath reaction. In brief, on a polished and cleaned silicon surface, a 300 nm Zn layer was deposited by RF magnetic sputtering method under an Ultimate Pressure of 1.0×10^{-3}Pa, Working Pressure of 3 Pa (Ar atmosphere) and sputter Power of 100 W. The specimen was then soaked in 70 ℃ warm water for 2 h.

Stearic acid and HTMS were used as modifier to lower the surface energy of these as-etched samples. To achieve superhydrophobic surfaces, as-prepared samples were directly dipped in a solution of 0.01 M stearic acid (the solvent is ethanol) for 15 min at ambient temperature to form a hydrophobic thin layer[28] (See Scheme 1). Meanwhile, an oleophobic surface (for oily liquids) could be achieved through HTMS modification by a thermal evaporation process [22] as follows: as-etched specimens and a bottle of 1mL HTMS solution (5 vol %, the solvent is isopropanol) were together sealed in a glass container, then placed in an oven at 85 ℃ for 3 h to reduce the surface energy (See Scheme 1).

On a drilled zinc surface (see ESI, FigS2a), a same growth and stearic acid modification process has also been introduced to form a superhydrophobic surface. While n-Hexane is used for the oil-water separation experiment.

2.3 Characterizations

The phase structure of the as-prepared samples was characterized by an X-ray diffractometer (XRD) (PHILIPS Corp., X'Pert PRO). The morphological structures were characterized by field emission scanning electron microscopy (FESEM, JSM-6700F). Fourier-transform infrared spectrometer (FTIR, 8700, Thermo Nicolet Co. USA) was used to characterize the surface chemistry. The surface chemical components were analysed using an X-ray photoelectron spectroscope (ESCALAB 250, Thermo-VG Scientific), equipped with Al-Kα radiation (hv=8047.8eV), the test depth was 3 nm. The water contact angle (WCA), water sliding angle (WSA), advancing and receding angle (AA and RA) were measured by the CAST2.0 contact angle analysis system (Solon Information Technology Co. Ltd., Shanghai, China) in ambient atmosphere (20 ℃). The volume of the individual water droplet in all measurements was 4 μL. The average WCA values were obtained by measuring the same sample at least on five different positions. WSA values were obtained by slanting the sample platform. The advancing and receding angle (AA and RA) were measured and recorded by holding the water droplet with a stationary needle in contact with the water surface and

moving the goniometer stage in one direction till the outline of the droplet changes[29]. Diiodomethane, formamide, diethylene glycol, and ethylene glycol were used to test the oleophobicity. The measured volume of oily liquid is 3.5 μL for formamide, diethylene glycol and ethylene glycol, and 1.5 μL for diiodomethane as its large density (3.32 g/ml).

3 Results and discussion

3.1 Phase structure characterization

The X-ray diffraction patterns for as-corroded zinc sheets are shown in Fig. 1. It is observed that after just acid etching, Zn diffraction peaks presented in Fig.1a perfectly coincide with JCPDS no.65-3358 and ICSD 52543. Through a two-step reaction, acid etch combined with warm water bath at 70 °C for 2 h, many new peaks corresponding to ZnO crystallographic planes appear in Fig.1b according to JCPDS no.36-1451 and ICSD 26170.

Usually, a naturally zinc hydroxide carbonate layer exists on the surface of zinc substrate. To eliminate its effect during just water bath process, we made a warm water soaking reaction on a sputtered Zn layer. The XRD patterns before and after water bath are shown in (ESI, Fig.S1a), It can be found the sputtered Zn film has good crystallinity, ZnO forms on the surface of Zn layer after water bath, the outstanding (100) and (002) peaks indicate a preferential ZnO radial growth, i.e. the formation of rod-like ZnO, which is similar with the situation of two-step approach. This tendency also can be found in the corresponding SEM images (ESI, Fig.S1b, 1c), while on the surface of the sputtered Zn grains, nanorods with a length of 100-300 nm,

diameter about 100 nm are formed as a result of water bath (in black circles in Fig.S1c).
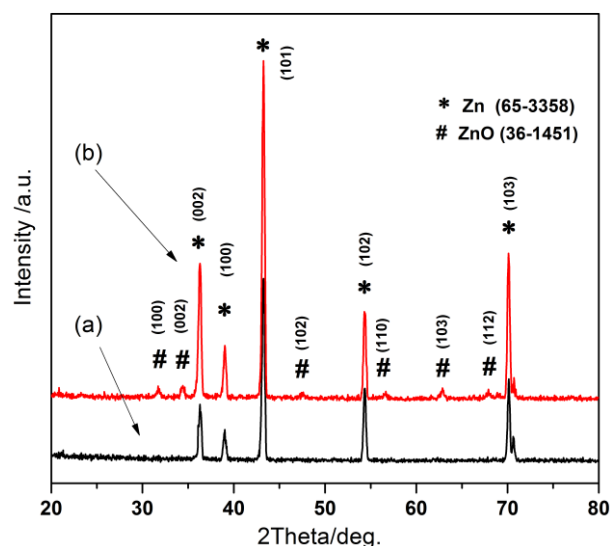
Fig.1 XRD images for as-prepared samples. XRD patterns for zinc sheet (a) with just HCl etch, and (b) with acid etch and water bath growth.

3.2 Surface morphological analysis, hydrophobic properties (for stearic acid modified interfaces) and growth mechanism exploration

After just being etched in hydrochloric acid, mountain-like grooves and ridges from over the entire surface (Fig.2a). The
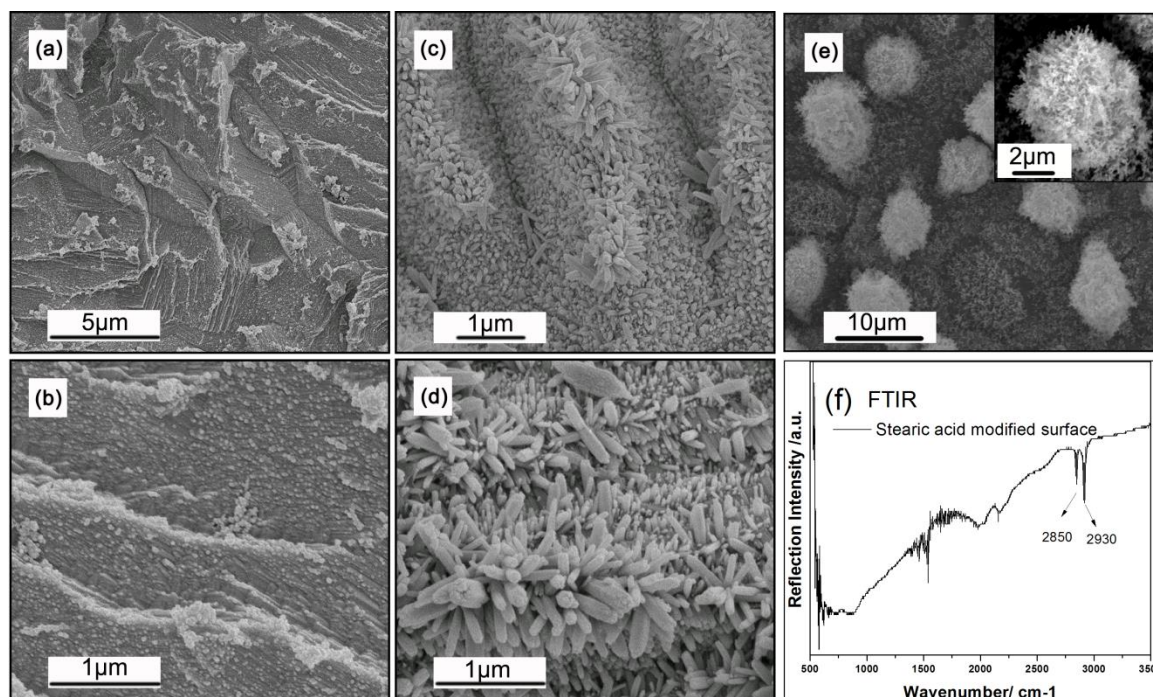
Fig.2 FESEM images of the zinc sheet surface with different treatments: (a) (b) with hydrochloric acid etching; (c) (d) with two-step growth; (e) the microstructure of lotus leaf surface; and (f) the FTIR image of stearic acid modified Zn/ZnO surface (by a two-step growth).
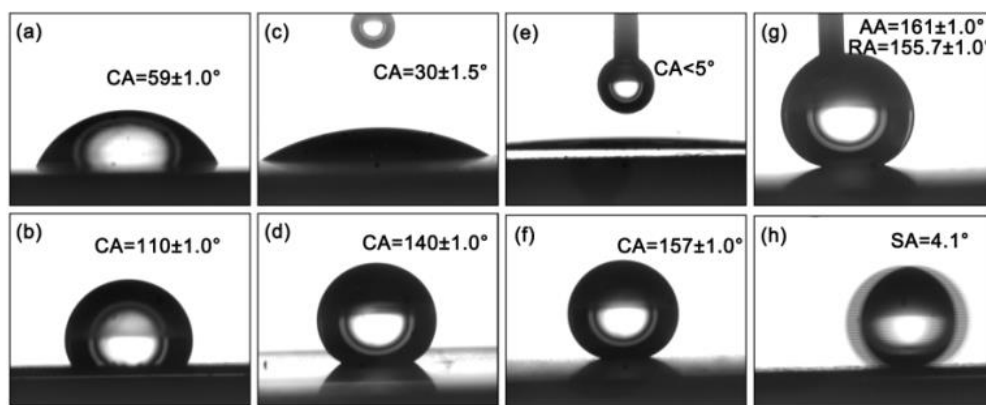
Fig.3 The wettability information of interfaces before and after stearic acid modification. The SCA of unmodified surface of (a) untreated Zn sheet, (c) HCl etched Zn surface, (e) HCl etched and water bathed Zn surface; (b) (d) (f) are the SCA of modified surface corresponding to (a) (c) (e) respectively. (g) (h) are CAH and SA of HCl etched and water bathed surface after modification.

width and depth of the grooves are 1-4 μm. From the prospective of the amplification (Fig.2b), a mass of Zn nano-protuberances distribute on the film surface, with a dimension from about 30 nm to 100 nm.

As a result of two-step reaction, combining acid etching with water bath growth, obvious hierarchical micro/nano microstructure appears on the zinc sheet surface (Fig.2c), with ZnO nanorods growing on the surface of micron-sized grooves and ridges. It can be found the micro topography is very similar to the hierarchical microstructure of the lotus leaf's surface with micron-sized bumps and nano-sized burrs (Fig.2e and the inset). The microtopography has been further observed in high-magnification image. From Fig.2d, it is observed that the length of the nanorods ranges from 100 nm to 1 μm, and the diameter for nanorods is less than 100 nm, in accordance with the size of the nanoparticles in Fig.2b. Thus, it can be deduced the Zn nano protuberances contribute to the subsequent growth of ZnO crystal.

Fig.2f is the infrared reflection spectrum on a stearic acid modified Zn/ZnO surface (two-step growth) measured by Fourier-transform infrared spectrometer, the absorption peaks located at 2850 cm^{-1} and 2930 cm^{-1} correspond to the vibration of $-CH_3$ and $-CH_2-$ group respectively, which indicates the stearic acid molecules are absorbed on the sample successfully. Note, the modification can't change the surface micromorphology as the stearic acid layer only exist on the surface at a thickness of several nano meters [28].

A modified hierarchical structure will be more helpful in realizing the surface superhydrophobic property [30, 31]. For hydrophilic Zn surfaces in Fig.3a and 3b, Wenzel Model is suitable to evaluate a rough factor "r", based the Wenzel equation[9],

$$Cos\ \theta_A = r \cos \theta\ \ (1)$$

Substitute the intrinsic contact angle θ_A =59 ° (Fig.3c) and apparent contact angle θ=30° (Fig.3a) to the equation, r~1.68 is acquired. While, r is the ratio between actual area and project area of the solid surface, apply the r value to evaluate the average title angle (α) of the grooves based on the equation:

$$Cos\ \alpha = project\ area/actual\ area=1/r\ \ (2)$$

We figure out the title angle is about 53.5 °, which seems to be matched to Fig.2c.

For a hydrophobic surface (modified by stearic acid), the higher the surface roughness, the more hydrophobic of the interface, even superhydrophobic. And this tendency is presented in Fig.3b, 3d and 3f, while the SCA ranges from 110 ° to 157 ° with the roughness increases.

The reason of the superhydrophobicity can be explained by Cassie-Baxter Model [10]. In Cassie's approach, when a liquid droplet contacts with a rough solid surface which possesses nanostructure or micro/nano hierarchical structures, air pockets exist between the water and the surface. The trapped air inside the grooves (including that between the nanorods) underneath the liquid contribute greatly to repelling the droplet, and the final apparent CA can be formulated as:

$$Cos\ \theta_A = f \cos \theta-(1-f) = f(1+ \cos \theta)-1\ \ (3)$$

Where θ_A is the apparent contact angle on a rough surface, while θ is the intrinsic contact angle on a corresponding flat surface, f is the area fraction of the solid/liquid interface, while (1-f) is the area fraction of the air/liquid interface.

The hierarchical micro/nano structure greatly reduces the contact area between liquid and solid, and a small value for f results in a larger contact angle θ_A. According to the results, θ=110 ° for stearic acid modified plane (shown in Fig.3b), θ_A = 157 ° for the stearic acid modified superhydrophobic surface (Fig.3f), the value of f is about 0.12, far below 0.39 for micrometer structure as θ_A = 140 ° (Fig.3d). The low contact area between water droplet and solid surface reduce the liquid adhesion, leading to a lower CAH (Fig.3g) and small SA (Fig.3h). The significance of hierarchical microstructure is outstanding. Simultaneously, it should be noted, without stearic acid modification, the hierarchical structured surface presents superhydrophilic (Fig.3e), water easily spreads on the surface, which is due to the high surface energy of ZnO. After modification, a superhydrophobic state appears (Fig.3f, g, h), which indicates the surface modification is indispensable. In summary, both high roughness and low surface energy are the necessary conditions to acquire a superhydrophobic interface.
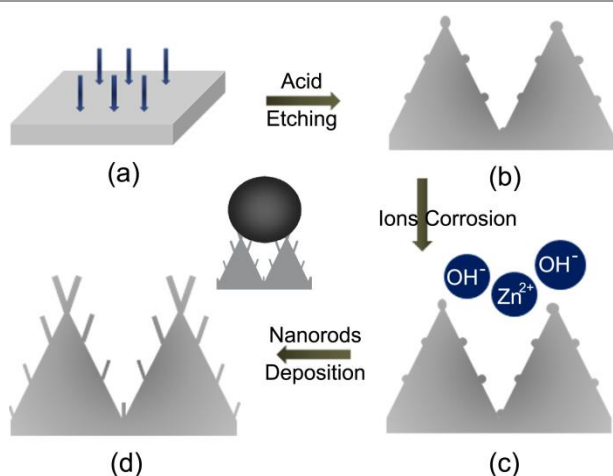
Fig.4 Schematic diagram for the formation process of hierarchical micro/nano configuration. The wetting state in theory is shown on the upper right corner of (d).

The formation mechanism of the hierarchical micro/nano structure is explained as Fig.4: micron-sized primary structure generates the first step of acid etch, with micron-grade configuration of mountain-like grooves and ridges (from Fig.4a to Fig.4b), which results from the anisotropic etch of the zinc substrate. What's more, the generated Zn nano protuberances play an important role for the subsequent ZnO growth. In warm water, zinc surface was attacked by hydrogen ions and part of zinc atoms turned into zinc ions (Fig.4c). When the ions concentration reached to a saturation value, zinc ions and hydroxyl ions would react to form ZnO molecules. The corresponding chemical equations are:

$$Zn + 2H^+ \rightarrow Zn^{2+} + H_2\uparrow \quad (4)$$

$$Zn^{2+} + 2OH^- \leftrightarrow ZnO + H_2O \quad (5)$$
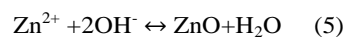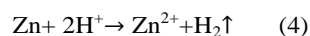
The generated ZnO crystal grains then deposited on the positions that etched by hydroxyl ions to form nanorods (Fig.4d), which is accordance with the XRD pattern in Fig.1b. These nano-sized Zn protuberances shown in Fig.2b possess high energy and occupy positive positions in chemical reaction, providing preferential locations for the growth of ZnO nanorods.

3.3 Effects of reaction temperature and duration on the microstructure and wettability

In the process of water bath, the effects of growth temperature and reaction duration on the ZnO microstructure have been systematically explored. Firstly, we set the water bath time as 2 h, hierarchical micro/nano structure can be formed at a temperature range from 50 ℃ to 90 ℃. When the temperature is as low as 50 ℃, shorter nanorods with a smooth surface are formed (Fig.5a). Raising the temperature to 90 ℃, the hierarchical structure is kept (Fig.5b), through a larger magnification, some hierarchical nanorods structure generate (Fig.5c), which originates from the severe corrosion of non-polar surface of ZnO nanorods and in situ deposition of vast ZnO particle under high temperature. While, the growth temperature is set at 70 ℃, the reaction time is changed from 0.5 h to 12 h. Fig.5d depicts a typical hierarchical configuration when the reaction time is 0.5 h, while the secondary structure of ZnO nanorods is still formed, with a smaller diameter and a casual and sparse distribution (Fig.5d). Extending the time to 12 h, cluster-like microstructures composed of nanotubes cover the surface (Fig.5e and 5f). The size of the flowers is about 10
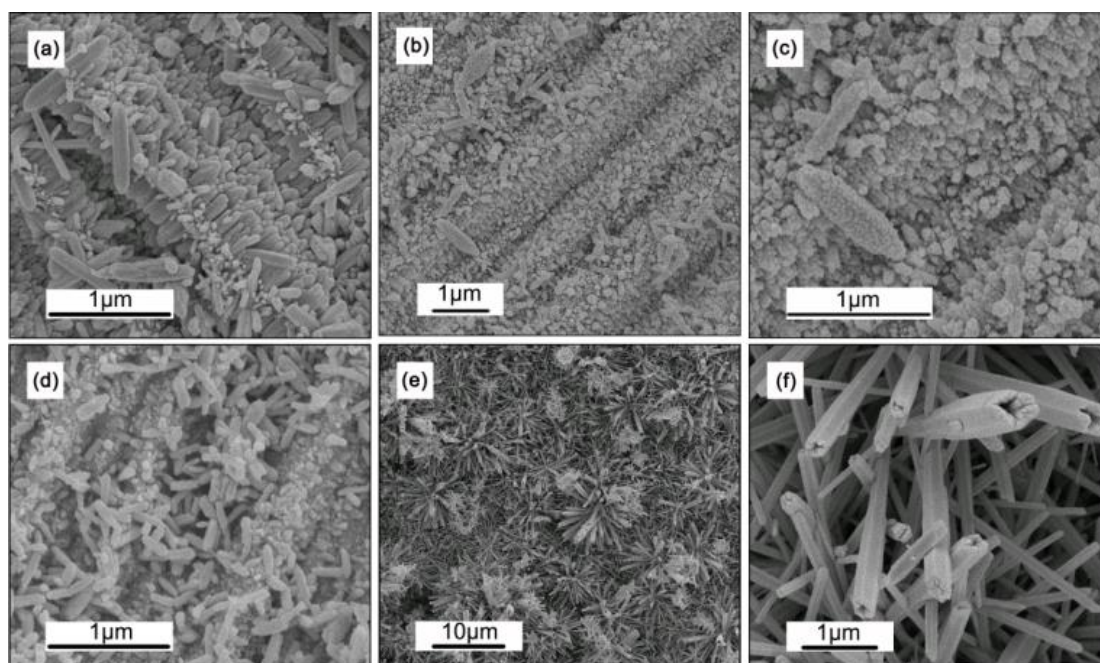
Fig.5 The resultant microstructures for samples under different water bath conditions. (a) 50 °C, 2 h; (b) (c) 90 °C, 2 h; (d) 70 °C, 0.5 h; and (e) (f) 70 °C, 12 h.

µm, and the length of nanotubes is about 3-5 µm. The formation of cluster-like structure originates from the apical growth dominance (the top of the Zn ridges can be sufficiently reacted with water), and the formation of ZnO nanotubes may be expounded as follows: the polar surface of zinc oxide possesses a higher energy, locating a metastable state, with a prolonged reaction time, the radial decomposition rate of the nanorods gradually exceeded the generation rate.

According to the above results, the Zn/ZnO hierarchical micro/nano microstructure can be easily obtained in a widespread experiment environment.

Table 1 Water wettability for samples generated in different warm water soaking conditions. The modifier is stearic acid.

Reaction condition	WCA (°)	WSA (°)	AA (°)	RA (°)	CAH (°)
50 ℃, 2 h	154±1	8.1	161.3	140.4	20.9
90 ℃, 2 h	152±1	10.0	162.1	150.1	12.0
70 ℃, 0.5 h	153±1	7.5	160.9	144.9	16.0
70 ℃, 2 h	157±1	4.1	161.0	155.7	5.3
70 ℃, 12 h	159±1	1.9	161.8	157.2	4.6

Table 1 is a summary of water droplets wettability on Zn/ZnO samples generated under various reaction temperature and duration. At a reaction time of 2h, 70 ℃ is a suitable temperature to generate a superhydrophobic interface because nanorods can grow to a suitable length and keep regular array. The generated interface under lower temperature (50 ℃) has a larger hysteresis, this is because the short and smooth nanorods lead to a larger contact area between the rods and water. And under a higher temperature reaction (90 ℃), the increased hierarchical ZnO nanorods can't offer a positive contribution in improving the wettability, because the tertiary ZnO nanoparticles are too small. Instead, the enlarged contact area between nanorods and water enhanced the adhesion, resulting in a large CAH and SA. Under 70 ℃ reaction, when the bath time is short, e.g. 0.5 h, these nanorods with random distribution induce the water droplet wetting on the surface tending to be a Wenzel state. A flower-like structure resulting from longer reaction duration, e.g. 12 h, greatly reduces the contact area between water and surface, leading to an excellent superhydrophobicity with a CA about 160 ° and SA tends to 0 °, which matches the condition of Cassie state. It indicates under a widespread reaction condition and surface modification, Zn/ZnO surfaces are endowed with hierarchical micro/nano configuration and superhydrophobicity. Reaction condition with temperature 70 ℃, time 2 h and stearic acid modification provides us a prefer choice to endow Zn substrate with superhydrophobic property in an economic and effective way.

3.4 Oleophobic properties (for HTMS modified interface)

While, the surface tension of stearic acid is near the oily liquids, to investigate the wettability in a further step, We modified the rough sample (acid corrosion and 70 ℃, 2h water bath) with a thin layer of HTMS ($CF_3(CF_2)_7(CH_2)_2Si(OCH_3)_3$) to study the
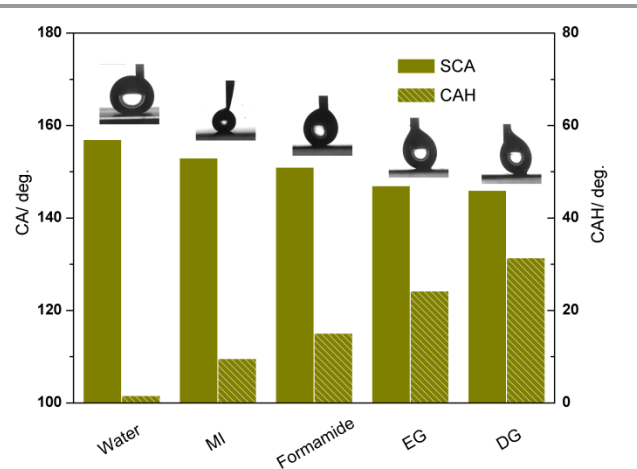
Fig.6 Wettability test result of oily liquids on HTMS modified surface.

Table 2 The surface tension information of some liquids for experiment and test.

Liquids in the experiment	Surface tension (m N/ m, 20 ℃)
water	72.80
diiodomethane	66.98
formamide	57.45
diethylene glycol	48.50
ethylene glycol	48.43
n-hexane	18.43
Stearic acid	33.40
HTMS	17.50

resistivity to oily liquids like the description in some literature[28]. The surface tension of HTMS is about 17.50 mN/m measured through a Capillary Rise Method under 20 ℃ environment, which is consistent with the low surface tension of functional groups –CF_3 (6 mN/m, 20 ℃) and –CF_2 (18 mN/m, 20 ℃). Some common used oily liquids are set as research objects, including diiodomethane (MI), formamide, diethylene glycol (DG), and ethylene glycol (EG). Surface tension information of these oily liquids is listed in Table 2. The static contact angle (SCA) and contact angle hysteresis (CAH) values are shown in Fig.6. Compared with a stearic acid modified surface (with CAH larger than 5 °), this HTMS modified surface presents an excellent superhydrophobicity with CAH less than 2 °. For diiodomethane and formamide, the SCA reaches over 150 °, and CAH are lower than 15 °, which meets the superoleophobic condition. However, CAH for different liquid droplets possesses huge difference though the SCA of different samples are close to each other, as seen from Fig.6, the CAH for diethylene glycol and ethylene glycol are larger than 20 ° while the SCA are near 150 °. While, the bigger of the surface tension difference between the liquid and the HTMS, the smaller of the CAH value, a different interaction between the liquid and the modified surface leads to a different three-phase contact line when liquid droplets stay on the surface. Both the micro topography and low surface energy of HTMS contribute to the good oleophobicity / superoleophobicity of the interface.

ARTICLE

3.5 Oil/water separation experiment (for stearic acid modified interface)

Motivated by oil/water separation experiment on copper meshes[32] and on stainless steel meshes[33, 34], we conduct a similar study on drilled Zn surface (acid corrosion and 70 ℃, 2h water bath) for the first time. The morphological image of Zn/ZnO drilled surface is shown in ESI, fig.S2. Restricted by our craft, the diameter (D) of the hole is 0.5 mm, and the aperture spacing (S) is 1.0 mm (ESI, fig.S2a). In a low magnification image in Fig.S2b, ZnO nanorods with irregular length spread on the wall of the hole. Fig.S2c is the enlarged image of the black circle region in Fig.S2b, the length of the nanorods ranges from 2 to 4 μm. which contributes to a superhydrophobic interface.

When the surface tension of the oil is lower than the solid surface, the wet behavior is happening, thus the stearic acid-modified copper meshes exhibit superoleophilic properties for n-hexane (18.43 mN/m, see Table 2). It can be clearly observed that the oil droplet quickly spreads on the mesh surface and permeates through the drilled holes freely, and then the oil droplet drops down easily if more oil is added (Movie S1). Simultaneously, superhydrophobic property is maintained. Water droplets can easily roll off the surface (Movie S2). The superoleophilic and superhydrophobic property contribute to the oil/water separation. In our experiments, water is dyed by methylene blue with a mass fraction 10ppm. The n-hexane/water separation phenomenon is shown in Movie S3. Oil/water mixture will be separated on the interface, water will flow over an oil lapped surface, while the drilled Zn sheet is fixed and the slant angle is set about 3 °. We define separation efficiency η= (m$_1$/m$_0$) ×100. Here, m$_0$ and m$_1$ were the mass of the oil (or the water) before and after separation process, respectively. After one time oil/water separation experiment, the surface was washed by ethanol and dried. The as-prepared interface can be repeatedly for more than 5 times and the separation efficiency kept over 90%. Some limitation exists in our crafts, more precision machining to reduce the diameter of the hole and decrease the pore spacing is in favour of larger separation efficiency.

3.6 Thermal stability test (for stearic acid modified interface)

Under engineering considerations, the thermal stability of the superhydrophobic samples (acid etching combined with warm water soaking at 70 ℃ for 2 h, stearic acid modification) have also been researched by heating the samples in air at different temperature for 4 h. The temperature ranges from 80 ℃ to 200 ℃ at an interval of 20 ℃. The SCA data for these treated samples presented in Fig.7. Superhydrophobic property is still maintained before the ambient temperature reaches to 200 ℃. In a common sense, stearic acid crystal has a melting point of 56-69.6 ℃, which is in contradiction with the high temperature stability. While, in our experiment, a thin layer of stearic acid molecules are attached on the ZnO surface to make the surface from superhydrophilic to superhydrophobic. The intimal
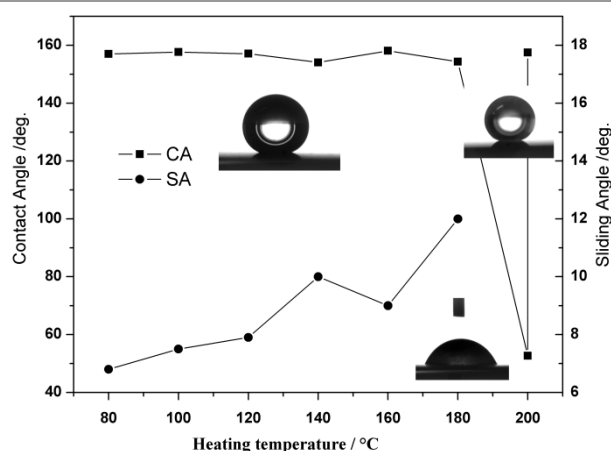
Fig.7 Thermal stability test results for stearic acid modified superhydrophobic surface.

Table 3. XPS result for superhydrophobic surface atom content change before and after185 ℃ heating.

Name	Zn2p3	O1s	C1s
Before	31.61%	34.65%	33.73%
after	41.45%	38.68%	19.87%

molecules are combined with the surface though a chemical bond which results from the reaction between the –COOH of the stearic acid and the –OH of the ZnO surface. The outer molecules are attached on the surface through Van der Waals forces among molecules. When the heating temperature is higher than the melting point, surface stearic acid molecules begin to disappear because of the weak Van der Waals forces, there is still some intimal molecules attaching on the ZnO surface since the strong chemical bonding energy. The analysis may be verified by the atom content change from the XPS result (Table 3), while the XPS has a 3 nm detect depth. Before heating, the atom content specific value (O-Zn)/C is about 1:10, which is near the value 1:9 in stearic acid. After heating in a 185° C for 4h, large amounts of O vacancies are generated, simultaneously, the specific value between C atom content and O atom content greatly deduces from 1.067 to 0.48. But there are still some stearic acid existing on the surface. More detail can be expounded from the XPS peak splitting maps for the sample heating at 185 ℃ (ESI, Fig.S3), the splitting peaks corresponding to C-C (284.6eV), C-H (285eV) and C=O (289eV) in C1s certify the existence of stearic acid molecules. Moreover, the lost superhydrophobicity resulting from high temperature (larger than 200 ℃) can be easily recovered by immersing the specimen into stearic acid again, as is shown in Fig.7.

3.7. Acid and alkali stability test
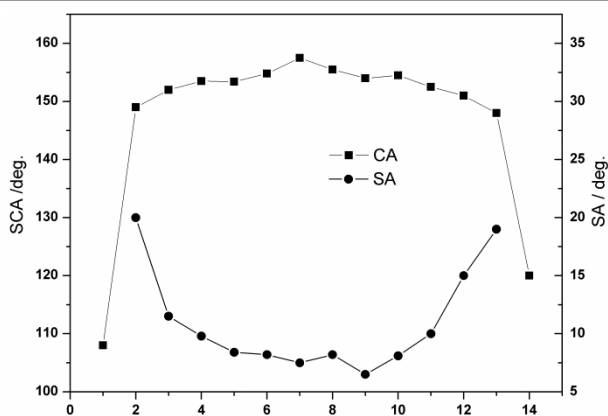
Fig.8 The PH stability test result of the superhydrophobic surface.

The wettability of water droplet with different PH value on the superhydrophobic surface (stearic acid modification) is shown in Fig.8. the surface can sustain its superhydrophobic property for water droplet with PH value from 4-11, with SCA> 150° and SA< 10° . With the increase of acidity or alkalinity, the anti-wettability decreases, especially to PH=1 and 14. In addition, we immerse the superhydrophobic sample in water with PH value from 5-9 for 1h. An immersion in water with PH=6 or PH=8 hardly affect the wettability, but the PH=5 or PH=9 environment will damage the anti-wettability. While the surface micromorphology hardly changes, thus it can be concluded the modifier is destroyed. In summary, the sample can't be easily corroded by water liquid with weak acidity or weak alkalinity because water can easily roll off from a inclined superhydrophobic surface, but it can't be immersed in these acid/ alkaline liquid for a long time.

4 Conclusions

In our study, a three step method, acid etch, water bath, and low surface energy modification has been introduced to construct Zn microgrooves/ ZnO nanorods superhydrophobic hierarchical structure. The greatest improvement is that the water itself acts as the reaction reagent without any additives. The superhydrophobicity or oleophobicity (for some oily liquids) have been researched respectively. Interestingly, on a drilled Zn surface, an oil/water separation experiment has been conducted, and the superhydrophobic interface with periodic holes is endowed with good oil/water separation property. What's more, these superhydrophobic samples present good thermal stability. The whole process to prepare superhydrophobic Zn/ZnO surface only need less than 3h (less than 1 min acid etch, 2h water bath and 15 min stearic acid modification) and the cost is so low since the available and inexpensive reaction reagents, which offer a way to prepared superhydrophobic materials in an industrial scale. However, this approach still faces some challenges: (1) disorder nanorods limit its theoretical simulation; (2) it is only suitable for limited kinds of active metals; (3) the harmfulness of Hydrochloric acid.

Notes and references

[a] Department of Physics, University of Science and Technology of China, Hefei 230026, China. Tel: 86 551 6360574; Email: xlxu@ustc.edu.cn (Xiaoliang Xu)
[b] Dalian Institute of Chemical Physics, Chinese Academy of Science, Dalian, Liaoning 116023, PR China.

Electronic Supplementary Information (ESI) available: [The XRD patterns and SEM image of sputtered Zn layer and Zn/ZnO composite structure after water bath process, The Zn/ZnO morphology on the Zn drilled holes treated by acid etch and water bath. The XPS spectrum for a heated superhydrophobic surface. Videos about superoleophilicity, superhydrophobicity and oil/water separation property of the drilled Zn sheet with Zn/ZnO microstructure.] See DOI: 10.1039/b000000x/

1. S. Wang and L. Jiang, *Advanced Materials*, 2007, **19**, 3423-3424.
2. X. Li, X. Du and J. He, *Langmuir*, 2010, **26**, 13528-13534.
3. X. Zhu, Z. Zhang, X. Xu, X. Men, J. Yang, X. Zhou and Q. Xue, *Journal of Colloid and Interface Science*, 2012, **367**, 443-449.
4. X. Deng, L. Mammen, H. J. Butt and D. Vollmer, *Science*, 2012, **335**, 67-70.
5. W. Liang and Z. Guo, *RSC Advances*, 2013, **3**, 16469-16474.
6. R. J. Daniello, N. E. Waterhouse and J. P. Rothstein, *Physics of Fluids*, 2009, **21**, 085103-085103-9.
7. M. He, J. J. Wang, H. L. Li and Y. L. Song, *Soft Matter*, 2011, **7**, 3993-4000.
8. X. Deng, L. Mammen, Y. F. Zhao, P. Lellig, K. Mullen, C. Li, H. J. Butt and D. Vollmer, *Advanced Materials*, 2011, **23**, 2962-2965.
9. R. N. Wenzel, *Ind. Eng. Chem.*, 1936, **28**, 988-994.
10. A. B. D. Cassie and S. Baxter, *T Faraday Soc*, 1944, **40**, 546-551.
11. J. Xi, L. Feng and L. Jiang, *Applied Physics Letters*, 2008, **92**, 053102-053102-3.
12. B. Zhang, J. Wang and X. Zhang, *Langmuir*, 2013, **29**, 6652-6658.
13. A. B. Djurisic, X. Liu and Y. H. Leung, *Physica Status Solidi-Rapid Research Letters*, 2014, **8**, 123-132.
14. J.-J. Wu, W.-P. Liao and M. Yoshimura, *Nano Energy*, 2013, **2**, 1354-1372.
15. I. Castro-Hurtado, G. G. Mandayo and E. Castano, *Thin Solid Films*, 2013, **548**, 665-676.
16. J.-I. Hahm, *Journal of Nanoscience and Nanotechnology*, 2014, **14**, 475-486.

RSC Advances Accepted Manuscript

17. I. Udom, M. K. Ram, E. K. Stefanakos, A. F. Hepp and D. Y. Goswami, *Materials Science in Semiconductor Processing*, 2013, **16**, 2070-2083.

18. M. Willander, O. Nur, Q. X. Zhao, L. L. Yang, M. Lorenz, B. Q. Cao, J. Z. Perez, C. Czekalla, G. Zimmermann, M. Grundmann, A. Bakin, A. Behrends, M. Al-Suleiman, A. El-Shaer, A. C. Mofor, B. Postels, A. Waag, N. Boukos, A. Travlos, H. S. Kwack, J. Guinard and D. L. S. Dang, *Nanotechnology*, 2009, **20**, 332001-332040

19. T. Darmanin, E. Taffin de Givenchy, S. Amigoni and F. Guittard, *Adv Mater*, 2013, **25**, 1378-1394.

20. X. M. Hou, F. Zhou, B. Yu and W. M. Liu, *Materials Science and Engineering a-Structural Materials Properties Microstructure and Processing*, 2007, **452**, 732-736.

21. M. Sakai, H. Kono, A. Nakajima, X. T. Zhang, H. Sakai, M. Abe and A. Fujishima, *Langmuir*, 2009, **25**, 14182-14186.

22. M. G. Gong, X. L. Xu, Z. Yang, Y. Y. Liu, H. F. Lv and L. Lv, *Nanotechnology*, 2009, **20**, 165602-165608.

23. M. Macias-Montero, A. Borras, Z. Saghi, J. P. Espinos, A. Barranco, J. Cotrino and A. R. Gonzalez-Elipe, *Nanotechnology*, 2012, **23**, 255303-255314.

24. X. Jinlei, F. Ke, S. Wenye, L. Kan and P. Tianyou, *Solar Energy*, 2014, **101**, 150-159.

25. S. T. Wang, L. Feng and L. Jiang, *Advanced Materials*, 2006, **18**, 767-770.

26. R. D. Narhe, W. Gonzalez-Vinas and D. A. Beysens, *Applied Surface Science*, 2010, **256**, 4930-4933.

27. Y. Chen, S. G. Chen, F. Yu, W. W. Sun, H. Y. Zhu and Y. S. Yin, *Surface and Interface Analysis*, 2009, **41**, 872-877.

28. H. Wang, J. Yu, Y. Wu, W. Shao and X. Xu, *Journal of Materials Chemistry A*, 2014, **2**, 5010-5017.

29. X. H. Chen, G. Bin Yang, L. H. Kong, D. Dong, L. G. Yu, J. M. Chen and P. Y. Zhang, *Crystal Growth & Design*, 2009, **9**, 2656-2661.

30. L. Feng, S. Li, Y. Li, H. Li, L. Zhang, J. Zhai, Y. Song, B. Liu, L. Jiang and D. Zhu, *Advanced Materials*, 2002, **14**, 1857-1860.

31. N. A. Patankar, *Langmuir*, 2004, **20**, 7097-7102.

32. Q. M. Pan, M. Wang and H. B. Wang, *Applied Surface Science*, 2008, **254**, 6002-6006.

33. C. F. Wang, F. S. Tzeng, H. G. Chen and C. J. Chang, *Langmuir*, 2012, **28**, 10015-10019.

34. D. Tian, X. Zhang, X. Wang, J. Zhai and L. Jiang, *Physical chemistry chemical physics : PCCP*, 2011, **13**, 14606-14610.